



A comparative study of the magnetocaloric effect in RNi_2 ($R = Dy, Ho, Er$) intermetallic compounds

E.J.R. Plaza^{a,b,*}, V.S.R. de Sousa^a, M.S. Reis^c, P.J. von Ranke^a

^a Instituto de Física 'Armando Dias Tavares', Universidade do Estado do Rio de Janeiro - UERJ, Rua São Francisco Xavier, 524, 20550-013, RJ, Brazil

^b Departamento de Física, Universidade Federal de Sergipe, 49100-000, São Cristóvão, Sergipe, Brazil

^c Instituto de Física, Universidade Federal Fluminense, Avenida Litorânea s/n, 24210-340, Niterói RJ, Brazil

ARTICLE INFO

Article history:

Received 4 March 2010

Received in revised form 13 May 2010

Accepted 21 May 2010

Available online 19 June 2010

PACS:

75.30.Sg

75.30.-m

75.30.Gw

Keywords:

Intermetallics

Anisotropy

Entropy

Magnetocaloric

Thermodynamic modeling

ABSTRACT

In this work we study the conventional and anisotropic magnetocaloric effects in the cubic rare-earth RNi_2 ($R = Dy, Ho, Er$) ferromagnetic intermetallic compounds. For each of these compounds we have explored the crystalline electrical-field anisotropy to predict the anisotropic magnetocaloric quantities under rotations of an applied magnetic field of constant intensity. The calculations were performed using proper parameters reported in the literature. Our results for the anisotropic magnetocaloric effect reveal some peculiarities of the spin reorientation which can be considered in designing new magnetocaloric materials for magnetic refrigerators.

© 2010 Elsevier B.V. All rights reserved.

1. Introduction

The magnetocaloric effect (MCE) is an exciting topic of investigation in the condensed matter physics field due to the link between magnetic and thermal properties of magnetic materials and its applicability in refrigeration technology [1]. The MCE is characterized by the release of heat as the result of the alignment of magnetic moments with an external applied magnetic field. It is usually characterized by the isothermal magnetic entropy change (ΔS_{mag}) and the adiabatic temperature change (ΔT_{ad}) which are conventionally observed under changes in the intensity of an external magnetic field (ΔH). In simple ferromagnets the maximum effect occurs around the Curie temperature (T_C) at which the magnetization changes most rapidly. In this respect, the MCE has been studied in several systems that undergo first-order or second-order phase transformations, including those ones that experience the influence of the magnetocrystalline anisotropy [1]. We shall refer to

the MCE obtained under variations in the intensity of the magnetic field with fixed orientation as *conventional* MCE.

In the field of MCE the study of magnetically anisotropic materials in single-crystalline form subjected to a relative rotation of the applied magnetic field of constant intensity (from one to another nonequivalent crystallographic direction) is of great importance. We shall refer to the MCE obtained under variations in the orientation of the magnetic field with fixed intensity as *anisotropic MCE* (AMCE). In this context, rare-earth based compounds such as the RNi_2 series offer the possibility of studying new characteristics of the MCE attached to their anisotropic behavior. Among them, the compounds with the largest free magnetic moment ($R = Tb, Dy, Ho, Er$) have been early studied in order to characterize their magnetothermal properties [2,3].

Most of the search for magnetic refrigerants has been guided by techniques focusing the conventional MCE. Since the discovery of the giant magnetocaloric effect (GMCE) in $Gd_5(Si_xGe_{1-x})_4$ systems [4,5] there is increasing interest in GMCE materials, in which the large ΔS is related to the first-order magnetic phase transition from ferromagnetic (FM) to paramagnetic (PM) coupled to a structural transformation. The drawback of the magnetic first-order phase transitions is the occurrence of hysteresis losses which were trying to be minimized, e.g. by subjecting a bulk material to fragmentation

* Corresponding author at: Universidade Federal de Sergipe, Departamento de Física, Av. Marechal Rondon, s/n Jardim Rosa Elze, CP 353 – 49100.000, São Cristóvão, SE, Brazil.

E-mail address: ejrplaza@gmail.com (E.J.R. Plaza).

[6] or by the partial modification of its composition [7].

Recently, we have proposed the use of the anisotropic MCE concomitantly with the conventional one in order to extend the operational temperatures in a thermal cycle that combines magnetic field intensity changes followed by rotation of the single-crystalline sample [8]. In fact, the idea of using anisotropic magnetic material in rotating thermal cycles was proposed by Kuz'min and Tishin [9]. By developing appropriate techniques, the complete process can be performed in materials showing first (or second) order-order or order-disorder magnetic transitions. It was also showed the possibility of achieving higher MCE exploring the magnetic anisotropy, in comparison with the FM-PM magnetic phase transition [10].

An important type of order-order magnetic transition is the spin reorientation transition (SR) as observed in some 4f-3d systems (with magnetic 3d transition elements). Recently, it has been shown the inability to explore the room-temperature SR for magnetic refrigeration in the referred systems [11], due to the predicted very small change in magnetic entropy. However, we claim that it is possible to find suitable values of ΔS (inclusive in the scope of the AMCE) in materials with non-magnetic partner of the rare-earth element around the SR. For instance, in DyAl₂ it was predicted higher MCE peaks in the anisotropic ΔS and ΔT around the SR temperature than in the conventional ΔS and ΔT around T_C [10].

In this paper we report a comparative study on the conventional and anisotropic MCE in RNi₂ (R = Dy, Ho, Er) intermetallics, in which the transition element has negligible magnetic contribution. In these ferromagnetic compounds the magnetic anisotropy comes mainly from the crystalline electrical field (CEF) acting on the rare-earth ions. For the calculations of the magnetic and magnetocaloric quantities in DyNi₂ and HoNi₂ the Zeeman, isotropic exchange and CEF interactions were included. In ErNi₂ we have also considered the quadrupolar interaction.

2. Theory

In the RNi₂ compounds, nickel ions practically have no magnetic moment but contribute to the establishment of the electronic structure and exchange interactions that leads to the FM arrangement of the localized R-magnetic moments. To calculate the magnetization as well as the magnetic entropy we consider the Hamiltonian

$$\hat{H} = \hat{H}_{\text{mag}} + \hat{H}_{\text{CEF}} + \hat{H}_{\text{Q}} \quad (1)$$

where

$$\hat{H}_{\text{mag}} = -g\mu_B [(H \cos \alpha + \eta M_x) \hat{J}_x + (H \cos \beta + \eta M_y) \hat{J}_y + (H \cos \gamma + \eta M_z) \hat{J}_z] \quad (2)$$

$$\hat{H}_{\text{CEF}} = W \left[\frac{X}{F_4} (\hat{\sigma}_4^0 + 5\hat{\sigma}_4^4) + \frac{(1-|X|)}{F_6} (\hat{\sigma}_6^0 - 21\hat{\sigma}_6^4) \right] \quad (3)$$

and

$$\hat{H}_{\text{Q}} = -G_1 (\langle \hat{\sigma}_2^0 \rangle \hat{\sigma}_2^0 + 3 \langle \hat{\sigma}_2^2 \rangle \hat{\sigma}_2^2) - G_2 (\langle \hat{P}_{XY} \rangle \hat{P}_{XY} + \langle \hat{P}_{YZ} \rangle \hat{P}_{YZ} + \langle \hat{P}_{ZX} \rangle \hat{P}_{ZX}) \quad (4)$$

are, respectively, the magnetic, CEF and quadrupolar interactions, written in an appropriate framework [12]. In relation (2), g is the Landé factor, μ_B the Bohr magneton, $\vec{H} = H(\cos \alpha, \cos \beta, \cos \gamma)$ the applied magnetic field, $\vec{M} = (M_x, M_y, M_z)$ the magnetization, η the exchange parameter and $\hat{J} = (\hat{J}_x, \hat{J}_y, \hat{J}_z)$ the total angular momentum vector operator. α, β and γ are the angles formed between the magnetic field vector and the x, y and z crystallographic axes, chosen as the [100], [010] and [001] crystallographic cubic directions,

respectively. In such coordinate system the CEF and quadrupolar terms [13] are indicated in relations (3) and (4), where F_4 and F_6 are dimensionless values tabulated for each R-element, W gives the CEF energy scale and $X (|X| \leq 1)$ gives the relative contributions of the fourth and sixth degree in O_n^m Stevens' equivalent operators [14]. $\hat{P}_{ij} = (\hat{J}_i \hat{J}_j + \hat{J}_j \hat{J}_i)/2$ and G_1 and G_2 are the quadrupolar parameters. From the calculated energy eigenvalues (ε_n) and eigenvectors ($|n\rangle$) of the Hamiltonian (1), the magnetization components M_δ ($\delta = x, y, z$) are obtained from the relation:

$$M_\delta = g\mu_B \frac{\sum_{n=1}^{2J+1} \langle n | \hat{J}_\delta | n \rangle e^{-\varepsilon_n/k_B T}}{\sum_{n=1}^{2J+1} e^{-\varepsilon_n/k_B T}}. \quad (5)$$

The intensity of the magnetization M and the component of the magnetization M_h along the applied magnetic field direction are $M = \sqrt{M_x^2 + M_y^2 + M_z^2}$ and $M_h = M_x \cos \alpha + M_y \cos \beta + M_z \cos \gamma$, respectively.

The total entropy can be written as the sum of the electronic, lattice (phonon) and magnetic parts, i.e. $S_{\text{tot}} = S_{\text{el}} + S_{\text{latt}} + S_{\text{mag}}$, where

$$S_{\text{el}}(T) = \bar{\gamma}T, \quad (6)$$

$$S_{\text{latt}} = -3R \ln \left[1 - \exp \left(-\frac{\Theta}{T} \right) \right] + 12R \left(\frac{T}{\Theta} \right)^3 \cdot \int_0^{\Theta/T} \frac{x^3 dx}{\exp(x) - 1} \quad (7)$$

and

$$S_{\text{mag}}(T, \vec{H}) = R \left(\frac{1}{k_B T} \frac{\sum_{n=1}^{2J+1} \varepsilon_n e^{-\varepsilon_n/k_B T}}{\sum_{n=1}^{2J+1} e^{-\varepsilon_n/k_B T}} + \ln \sum_{n=1}^{2J+1} e^{-\varepsilon_n/k_B T} \right). \quad (8)$$

One can use Eqs. (6)–(8) to calculate the quantities that characterize either the conventional or anisotropic MCE. In the conventional MCE, i.e. fixing the magnetic field at an arbitrary direction and changing its intensity from H_i to H_f , we have

$$\Delta S^{[\cos \alpha_a, \cos \beta_a, \cos \gamma_a]}(T, H) = S^{[\cos \alpha_a, \cos \beta_a, \cos \gamma_a]}(T, H_f) - S^{[\cos \alpha_a, \cos \beta_a, \cos \gamma_a]}(T, H_i) \quad (9)$$

and

$$\Delta T^{[\cos \alpha_a, \cos \beta_a, \cos \gamma_a]}(T, H) = T^{[\cos \alpha_a, \cos \beta_a, \cos \gamma_a]}(S_{\text{tot}}, H_f) - T^{[\cos \alpha_a, \cos \beta_a, \cos \gamma_a]}(S_{\text{tot}}, H_i), \quad (10)$$

where the set of angles $[\alpha_a, \beta_a, \gamma_a]$ defines an arbitrary direction in respect to the x, y and z crystallographic axes. Now it is convenient to define the set of angles $[\alpha_e, \beta_e, \gamma_e]$ to the easy magnetization direction in respect to the same frame. In the anisotropic MCE, i.e. fixing the magnetic field intensity and changing its direction from $(\alpha_e, \beta_e, \gamma_e)$ to $(\alpha_a, \beta_a, \gamma_a)$, we have

$$\Delta S_{\text{an}}(T, H) = S^{[\cos \alpha_a, \cos \beta_a, \cos \gamma_a]}(T, H) - S^{[\cos \alpha_e, \cos \beta_e, \cos \gamma_e]}(T, H) \quad (11)$$

and

$$\Delta T_{\text{an}}(T, H) = T^{[\cos \alpha_a, \cos \beta_a, \cos \gamma_a]}(S_{\text{tot}}, H) - T^{[\cos \alpha_e, \cos \beta_e, \cos \gamma_e]}(S_{\text{tot}}, H) \quad (12)$$

If the magnetic field does not alter neither the Sommerfeld coefficient ($\bar{\gamma}$) nor the Debye temperature (Θ), the total entropy change (in an isothermal process) is equal to the magnetic entropy change ($\Delta S_{\text{tot}} = \Delta S_{\text{mag}}$). From experimental (or theoretical) magnetization or specific heat data, it is frequent the use of the relations: $S_{\text{mag}}(T, H_i) - S_{\text{mag}}(T, H_f) = \int_{H_i}^{H_f} -(\partial M / \partial T)_H dH$ (Maxwell's relation) or $S_{\text{tot}}(T, H) = \int_0^T T^{-1} C(T, H) dT$ to obtain the conventional $\Delta S_{\text{mag}}(T)$ and $\Delta T_{\text{ad}}(T)$ curves ($C(T, H)$ being the specific heat). In the

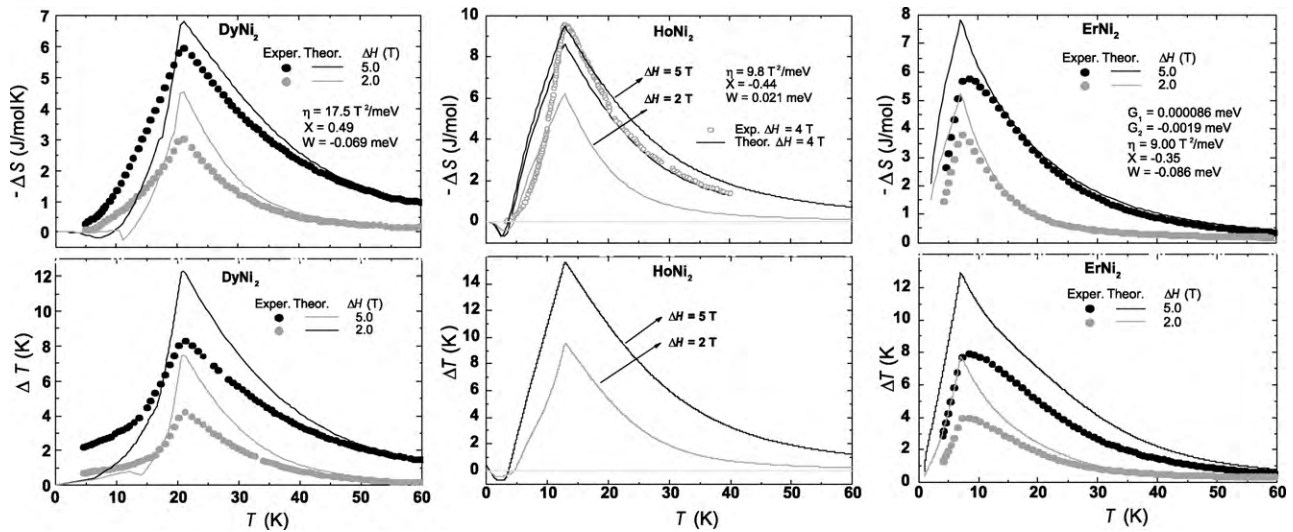


Fig. 1. Temperature dependence of the conventional MCE, ΔS and ΔT in RNi_2 ($R=Dy, Ho, Er$) compounds for $\Delta H=2$ and 5 T. The calculations were performed considering the average ΔS and ΔT in the main cubic crystallographic directions. Experimental data for polycrystalline samples are included.

anisotropic case we have previously studied various R–X type compounds with X non-magnetic [8] and the results showed the same as those obtained from the corresponding Maxwell's relation [15].

For the calculations of isotropic S_{el} and S_{latt} of the RNi_2 compounds we use a common value for the electronic heat capacity coefficient, $\bar{\gamma} = 5.4 \text{ mJ mol}^{-1} \text{ K}^{-1}$, and interpolated effective Debye temperature Θ -values from the non-magnetic $LaNi_2$ and $LuNi_2$ compounds [16]. It should be noticed that in this model the anisotropy corresponds to the magnetic part of the total entropy.

3. Application and discussion

In the following we will apply the above theoretical considerations to study the conventional and anisotropic MCE in the $DyNi_2$, $HoNi_2$ and $ErNi_2$ compounds. In order to perform the calculations, we consider the model parameters listed in Table 1.

The conventional MCE in the RNi_2 series has been studied by von Ranke and co-workers and their results were published in some early reports [16,20,21]. For the $DyNi_2$ compound we consider [001] as the easy axis [22] instead of the [111] one which follows from the considered set of parameters $X=-0.10$, $W=-0.019$ and $\eta = 15.5 \text{ T}^2/\text{meV}$ in Ref. [16]. For the $HoNi_2$ compound, instead of the [001] easy axis indicated in Ref. [20], the common set of parameters included in Table 1 lead to a [110] easy axis of magnetization (see also Ref. [21]). In the same reference, for the $ErNi_2$ compound there is a misleading in the reported CEF parameters being corrected here, see Table 1, where we have additionally included the quadrupolar parameters.

Since these compounds show easy axis in the plane defined by [001] and [110] directions, we will consider magnetic fields also in this plane for the calculations of anisotropic MCE. Then, it is useful to define the angle between the magnetization and the [001] polar-axis: $\theta = \tan^{-1}(\sqrt{M_x^2 + M_y^2}/M_z)$, since in the calculations we restrict the magnetization in the referred plane.

Table 1

Crystalline electrical field, exchange and quadrupolar parameters, easy axis direction (*e. a.*) and Curie temperatures for the $DyNi_2$, $HoNi_2$ and $ErNi_2$ compounds.

Compound	X	W (meV)	η (T^2/meV)	G_1 (meV)	G_2 (meV)	<i>e. a.</i>	T_C (K)	Ref.
$DyNi_2$	0.49	-0.069	17.5	–	–	[001]	21	[16]
$HoNi_2$	-0.44	0.021	9.8	–	–	[110]	13	[17,18]
$ErNi_2$	-0.35	-0.086	9.0	8.6×10^{-5}	-0.0019	[001]	7	[19]

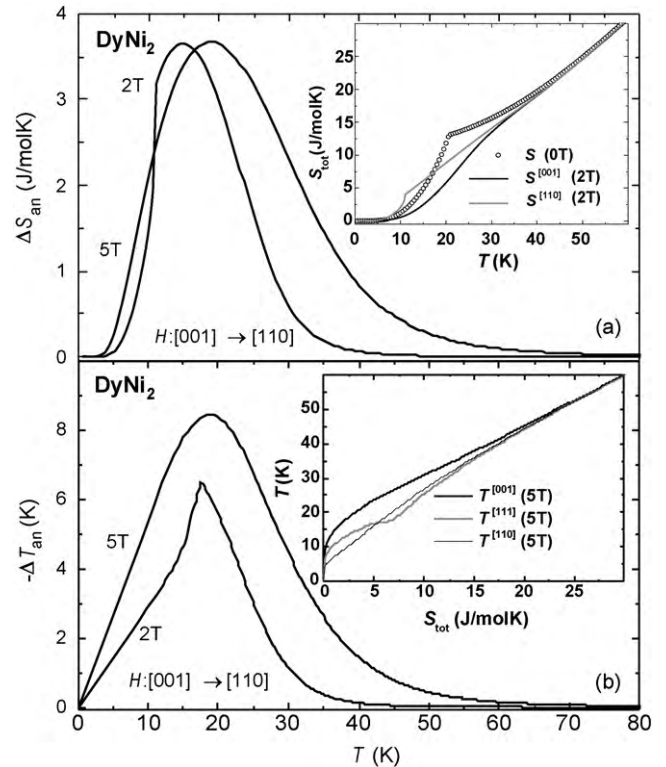


Fig. 2. Theoretical anisotropic curves for ΔS_{an} (a) and ΔT_{an} (b) in $DyNi_2$ compound for the magnetic field directional changes from [001] to [110] with fixed intensities of 2 and 5 T. The insets show the calculated $S_{tot}(T)$ for $H=2$ T ([001] and [110] directions) and $T(S_{tot})$ for $H=5$ T ([001], [111] and [110] directions). The $S_{tot}(T)$ curve in absence of field is also showed.

The top and bottom panels in Fig. 1 show the calculated conventional ΔS and ΔT curves, respectively. Experimental curves (from specific heat measurements) for the magnetic field variation from 0 to 2 T and 0 to 5 T were taken from Ref. [16] for DyNi₂ and from Ref. [20] for ErNi₂. In the HoNi₂ case the experimental ΔS curve corresponds to a field variation from 0 to 4 T and was taken from Ref. [18].

Since the experimental curves come from polycrystalline samples the results correspond to an average over all of the possible directions. An appropriate average of the calculations over the three symmetry axes $(\Delta S^{[001]} + \Delta S^{[110]} + \Delta S^{[111]})/3$ and $(\Delta T^{[001]} + \Delta T^{[110]} + \Delta T^{[111]})/3$ gives practically the same results as the more sophisticated method of Ayant et al. [23]. The exchange parameters were slightly adjusted in order to reproduce accurately the peak positions and the agreement between experimental and calculated results is satisfactory, as we see in Fig. 1. As in NdNi₂ and TbNi₂ [8], differences between observations and calculations can be due to structural and compositional inhomogeneities as well as the existence of defects in the polycrystalline samples. In respect to the CEF parameters it should be taken into account that RNi₂ compounds crystallize in a derived Laves-phase superstructure [24].

We discuss now the main contributions and results of our paper, i.e., the anisotropic MCE in the selected RNi₂ compounds. Fig. 2(a) and (b) shows, respectively, the anisotropic ΔS_{an} and ΔT_{an} curves of DyNi₂ calculated for magnetic fields of 2 and 5 T which orientation was changed from the [001] towards the [110] direction. The ΔS_{an} and ΔT_{an} curves were obtained from relations (11) and (12), by means of the difference of the isothermal and isentropic differences between the curves shown in the insets of Fig. 2. Note from the inset in Fig. 2(a) that the curve with the magnetic field applied in the [110] direction shows higher entropy than the one calculated at zero magnetic field below 17 K, above which the opposite behavior is observed. This is a consequence of anisotropy and a field-induced spin reorientation transition (SR) at $T_{SR} = 11$ K. The SR transitions are dependent on the intensity of the applied magnetic field and on its relative orientation in respect to the crystallographic axis. Note from the inset in Fig. 2(b) the kink observed for the [111] direction, revealing the SR at $T_{SR} = 17.5$ K for $H = 5$ T.

Fig. 3(a) and (b) displays, respectively, theoretical results of $\theta(T, H)$ and ΔS_{an} for the HoNi₂, showing characteristics of the field-induced SR transitions in this compound. As we see in Fig. 3(a), at low temperatures and low fields, $\theta \sim \pi/2$ indicates the [110] direction as the easy axis of magnetization. One can observe an abrupt decrease in the polar θ -angle either at zero-field or not very intense magnetic field along the [001] direction. In the intermediate field region (e.g. 0.05 and 0.1 T) the $\theta(T)$ curves reveal clearly a first-order SR transition followed by a second-order SR-alignment of the magnetization to the direction of the applied field (see inset), i.e. when $M = M_h$.

Theoretical results for $\Delta S_{an}(T)$ in HoNi₂ with [110] to [001] field rotation and intensities 0.5 and 1 T is shown in Fig. 3(b). For $H = 0.5$ T one observe a table-like shape of the entropy change. Also, the peak intensity at T_{SR} (marked by arrows) suggests its increasing with the field intensity. The inset shows the calculated $S_{mag}(T)$ in zero field and for $H = 0.5$ T along the [001] and [110] directions.

In Fig. 4, we show theoretical results for anisotropic $\Delta S_{an}(T)$ curves of the ErNi₂ compound for magnetic field variation from [001] to [110] directions and selected intensities. One can observe a diminution of the $\Delta S_{an}(T)$ intensity-peak as the field increases from 0.1 to 1 T and a reverted signal (the inverse MCE) when larger fields are used. This is due to the spin reorientation effects, which are dependent on the direction and intensity of the applied magnetic field. Note the clear first-order SR transition for the $H = 0.3$ T curve at 2.8 K approximately.

Different from the approach reported in Ref. [25], we investigated here the influence of magnetic field change direction

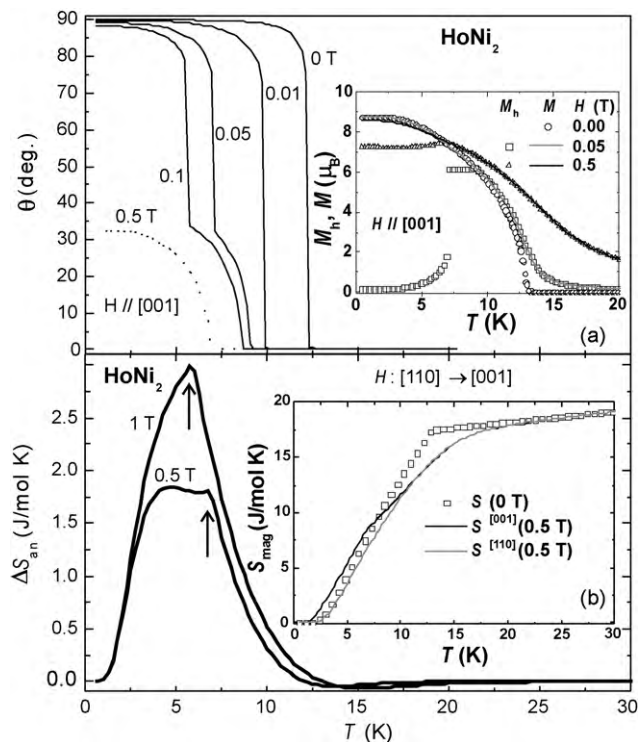


Fig. 3. Theoretical $\theta(T)$ (a) and $\Delta S_{an}(T)$ (b) curves for the HoNi₂ compound. Arrows indicate the SR-alignment temperatures of the magnetization to the [001] direction. The insets show the calculated magnetization M and the component of the magnetization M_h along the applied magnetic field [001]-direction as well as the magnetic entropy contributions.

(constant intensity) on the anisotropic magnetic compounds (RNi₂ cases). There are other approaches oriented to optimize the magnetocaloric response of the RNi₂ magnetic material such as the partial substitution of Ni by a magnetic element [26]. This can lead to new perspectives about the role of the spin reorientation in the anisotropic magnetocaloric effect.

The anisotropic entropy change for the selected RNi₂ compounds has been calculated directly by using Eq. (8). Experimentally, through magnetization data of single-crystalline sample, one can obtain the usual magnetocaloric effect for two directions (using the same magnetic field variation) in such a way that $\Delta S_{an}(T)$ is obtained by difference. This is due to the fact that entropy at zero-field (or very small field) is practically insensitive to the direction of the applied magnetic field. Another way to obtain $\Delta S_{an}(T)$ is

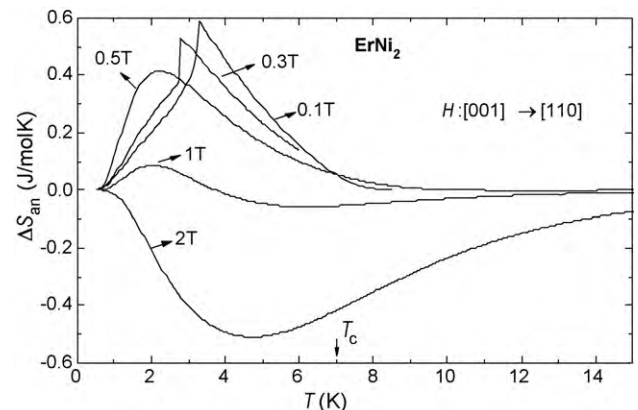


Fig. 4. Theoretical anisotropic ΔS_{an} curves of the ErNi₂ compound for magnetic field variation from [001] to [110] directions and selected intensities.

by measurements of the isoangle transversal component of the magnetization at fixed intensity field as deduced by some of us [15]. Despite the lack of magnetic data for these compounds in single-crystalline form, we can predict the anisotropic behavior based on the model parameters and experimental results for polycrystalline samples. Nevertheless, it is desirable efforts to prepare and characterize rare-earth based single crystals (R–X type with X non-magnetic) in order to study more accurately the details of the anisotropic magnetocaloric effect.

4. Conclusion

We studied the conventional and anisotropic magnetocaloric effect in RNi₂ compounds (R=Dy, Ho, Er). The correctness of the model parameters was checked by fitting experimental results found in the literature (conventional ΔS and ΔT curves), and therefore they were used to calculate the anisotropic behavior of the MCE (ΔS_{an} and ΔT_{an} curves). Our predictions for the anisotropic case revealed some peculiarities of the spin reorientation which can be useful for practical applications. Depending on the order of the transition and the separation between T_C and T_{SR} temperatures, the magnetocaloric curves can show either sharp-lambda or table-like type profiles. An interesting observation is the decreases of the $\Delta S_{an}(T)$ -peak when the intensity of magnetic field increases (as calculated for the Dy and Er for some symmetry cases). Additionally, for the ErNi₂ compound the use of larger fields induces a partial or total reverted signal (the inverse MCE) of the $\Delta S_{an}(T)$ curves. We expect this study contributes to stimulate the realization of magnetic measurements in rare-earth based single crystals in order to check for adequate compound to be used as anisotropic refrigerant materials.

Acknowledgments

The authors are grateful to the Fundação de Amparo à Pesquisa do Estado de Rio de Janeiro (Faperj) and to the Conselho Nacional de

Desenvolvimento Científico e Tecnológico (CNPq) for the financial support.

References

- [1] A.M. Tishin, Y.I. Spichkin, *The Magnetocaloric Effect and its Applications*, Taylor & Francis, Bristol, 2003.
- [2] A. Tomokiyo, H. Yayama, H. Wakabayashi, T. Kuzuhara, T. Hashimoto, M. Sahashi, K. Inomata, *Adv. Cryog. Eng.* 32 (1986) 295.
- [3] H. Yayama, A. Tomokiyo, T. Hashimoto, T. Kuzuhara, R. Li, M. Sahashi, K. Inomata, *IEEE Trans. Magn.* 23 (1987) 2850.
- [4] V.K. Pecharsky, K.A. Gschneidner Jr., *Phys. Rev. Lett.* 78 (1997) 4494.
- [5] V.K. Pecharsky, K.A. Gschneidner Jr., *Appl. Phys. Lett.* 70 (1997) 3299.
- [6] J.D. Moore, G.K. Perkins, Y. Bugoslavsky, M.K. Chattopadhyay, S.B. Roy, P. Chad-dah, V.K. Pecharsky, K.A. Gschneidner Jr., L.F. Cohen, *Appl. Phys. Lett.* 88 (2006) 072501.
- [7] Virgil Provenzano, Alexander J. Shapiro, Robert D. Shull, *Nature* 24 (2004) 853.
- [8] E.J.R. Plaza, V.S.R. de Souza, P.J. von Ranke, A.M. Gomes, D.L. Rocco, J.V. Leitão, M.S. Reis, *J. Appl. Phys.* 105 (2009) 013903.
- [9] M.D. Kuz'min, A.M. Tishin, *J. Phys. D: Appl. Phys.* 24 (1991) 2039–2044.
- [10] P.J. von Ranke, N.A. de Oliveira, E.J.R. Plaza, V.S.R. de Souza, B.P. Alho, A. Magnus, G. Carvalho, S. Gama, M.S. Reis, *J. Appl. Phys.* 104 (2008) 093906.
- [11] Michael D. Kuz'min, Manuel Richter, *Appl. Phys. Lett.* 90 (2007) 132509.
- [12] H.G. Purwins, A. Leson, *Adv. Phys.* 39 (1990) 309.
- [13] K.R. Lea, M.J.M. Leask, W.P. Wolf, *J. Phys. Chem. Solids* 33 (1962) 1381.
- [14] K.W.H. Stevens, *Proc. Phys. Soc. A* 65 (1952) 209.
- [15] E.J.R. Plaza, V.S.R. de Souza, B.P. Alho, P.J. von Ranke, *J. Alloys Compd* (2010), doi:10.1016/j.jallcom.2010.05.044.
- [16] P.J. von Ranke, V.K. Pecharsky, K.A. Gschneidner Jr., *Phys. Rev. B* 58 (1998) 12110.
- [17] E.A. Goremychkin, I. Natkaniec, E.M. Muhle, D. Chistyakov, *J. Magn. Magn. Mater.* 81 (1989) 63.
- [18] A.M. Gomes, I.S. Oliveira, A.P. Guimarães, A.L. Lima, P.J. von Ranke, *J. Appl. Phys.* 93 (2003) 6939.
- [19] D. Gignoux, F. Givord, *J. Magn. Magn. Mater.* 31–34 (1983) 217.
- [20] P.J. von Ranke, E.P. Nóbrega, I.G. de Oliveira, A.M. Gomes, R.S. Sarthour, *Phys. Rev. B* 63 (2001) 184406.
- [21] P.J. von Ranke, E.P. Nóbrega, I.G. de Oliveira, A.M. Gomes, R.S. Sarthour, *J. Alloys Compd.* 344 (2002) 145.
- [22] D. Gignoux, F. Givord, *Solid State Commun.* 21 (1977) 499.
- [23] Y. Ayant, E. Belorizky, M. Guillot, J. Rosset, *J. Phys. (Paris)* 26 (1965) 385.
- [24] A. Lindbaum, E. Gratz, S. Heathman, *Phys. Rev. B* 65 (2002) 134114.
- [25] A.L. Lima, K.A. Gschneidner Jr., V.K. Pecharsky, *J. Appl. Phys.* 96 (2004) 2164.
- [26] Niraj K. Singh, S. Agarwal, K.G. Suresh, R. Nirmala, A.K. Nigam, S.K. Malik, *Phys. Rev. B* 72 (2005) 14452.